

TWO COMPLEMENTARY APPROACHES TO MODELLING A BIOSENSOR

N. D. Botkin, O. A. Pykhiteev, B. N. Starovoitova, V. L. Turova
Center of Advanced European Studies and Research (caesar)
Ludwig-Erhard-Allee 2, 53175 Bonn, Germany
e-mail: pykhiteev@caesar.de

K.-H. Hoffmann
Technical University of Munich
Boltzmannstr. 3, 85747 Garching, Germany

ABSTRACT

The paper outlines two approaches to the modelling of a biosensor which serves for the detection and quantitative measurement of microscopic amounts of biological substances. The operation principle of this device is based on the excitation, propagation, and detection of acoustic surface shear waves in a multilayered structure that contacts a fluid containing a protein to be detected. The mathematical model of such a structure involves large systems of coupled partial differential equations that describe piezoelectric, elastic, and hydrodynamic properties of the structure. Because of the short wavelength, the implementation of such a model with finite elements in three dimensions requires a very fine mesh and, therefore, forces to use parallel computing. Thus, it would be useful to have a simple tool for a fast preliminary analysis which would provide information about the structure of solutions. The paper presents such a tool developed using harmonic analysis techniques that are based on the construction of travelling wave solutions in the multilayered structure of the biosensor under assumption that the structure is unbounded in horizontal and downward directions. These assumptions are reasonable because the real biosensor chip is embedded up to the surface into a very viscous damping medium to exclude the reflection of waves on side and bottom faces, which imitates the above mentioned unboundedness.

KEY WORDS

Love wave biosensor, multi-layered structures, dispersion relations, surface acoustic waves

1 Introduction

The object of the modelling is a biosensor that serves for the measurement of small amounts of diverse biological substances in liquids. It can be considered as a multi-layered structure (see Figure 1) whose bottom layer is an ST-cut of piezoelectric α -quartz. Acoustic shear waves are excited here by means of alternate voltage applied to electrodes deposited on it. The waves are transmitted into a thin film, isotropic guiding layer, deposited on the top of the substrate. The top gold layer is covered by tiny receptors, aptamers, which are able to bind proteins from the contacting liquid specifically. When protein molecules adhere to the receptors, the additional mass causes a phase shift in the electric signal which is measured on the output electrodes.

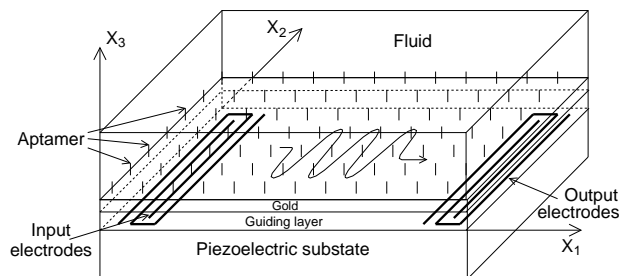


Figure 1. Sketch of a biosensor

A high sensitivity regarding to the mass loading is achieved due to the usage of shear horizontally polarized guided waves (Love waves) because of their low interaction with the contacting fluid. The input and output electrodes are located between the substrate and the guiding layer. To obtain purely shear polarized modes with the displacements parallel to the x_2 -axis, the direction of the wave propagation is chosen to be orthogonal to the crystalline X -axis. The choice of materials must ensure that the wave velocity in the guiding layer is less than the one in the substrate so that the waves will be transferred into the guiding layer. We state a three-dimensional mathematical model that describes the biosensor structure consisting of five coupled layers: three solid layers with different elastic and electric properties, a bristle-like aptamer layer and a liquid layer considered as a weakly compressible viscous fluid. Full coupling between the deformation and electric fields is assumed. Thus, the presented model is an extension of the model described in [1].

The bristle-like aptamer layer cannot be modelled directly using liquid-solid interface conditions because the number of aptamer molecules is giant whereas their thickness is very small. A special homogenization technique described in [2] enables to reduce the problem to the case a bulk layer. According to this technique, the original aptamer-fluid structure is replaced by an averaged material whose properties are derived as the number of aptamer molecules goes to infinity whereas their thickness goes to zero but the height remains constant. Thus, we end up with a new bulk layer whose thickness is equal to the height of the aptamer molecules and whose behavior is described by limiting equations.

The presented paper discusses two complementary

approaches for the treatment of the basic model. These are finite element (FE) method and harmonic analysis based on the construction of travelling wave solutions in a relaxed model. The FE-approach provides accurate results because of accounting for the exact parameters of the sensor such as the shape of the electrodes, their position, mass, electro-conductivity properties. This allows us to estimate important characteristics of the biosensor and effects caused by scattering of waves.

The FE-model presented in this paper extends the one described in [1] by additionally considering the gold layer and the homogenized one that models the aptamer-liquid structure. The model is numerically implemented with the FE-program FeliCs developed at the Technical University of Munich. The sparse linear algebra is supported by a parallelized version of the library SPOOLES (see [3]). A MAPLE-code for the automatic derivation of the model equations is developed. This code computes the total energy and its variations in a symbolic form. This yields the model equations in a form appropriate for the input of FeliCs.

The main difficulty of implementation of the FE-approach is very high resource-consuming due to a very small wavelength. A large number of elements in x_1 -direction is required to resolve the wave structure. The number of degrees of freedom lies in the range of 10^7 - 10^8 , which makes impossible simulations on stand-alone ordinary computers and requires parallel computing.

Another approach is related to the harmonic analysis developed in [5], which provides a method to construct travelling wave solutions feasible in the biosensor structure under assumption that the last is unbounded in the lateral and downward directions. Such an assumption is very realistic because real biosensor chips are imbedded up to the surface in very viscose damping media to exclude the reflection of waves on the side and bottom faces. To some extent, this is equivalent to the above mentioned acoustic unboundedness.

The method can treat multi-layered structures consisting of layers of different nature including piezoelectric, isotropic, bristle-like, and liquid layers, which is sufficient for the modelling of the biosensor. The structure assumes to be unbounded and homogeneous in the lateral directions. So that the electrodes cannot be taken into account. The top and bottom layers may be either semi-infinite in the vertical direction or they may contact with media such as fluids, gases or vacuum. These simplifications prevent this method from the accurate simulation of the biosensor. Nevertheless, it can provide very important preliminary information such as the wavelength and the displacement profile in the transversal direction including the attenuation rates of waves in the substrate and in the fluid. Such information is very important for choosing optimal reliable finite element approximations. Another advantage of this method is its computational efficiency: the runtime on a common personal computer lies in the range of seconds.

Thus, the following scheme of modelling is proposed.

First, the travelling wave harmonic analysis is being applied, which yields the wavelength and the transversal profile of displacements and, therefore, the attenuation rate of waves in the substrate (downward) and the fluid (upward). This information is then used to formulate requirements on the finite element mesh and to introduce special elements whose shape functions decay according to the attenuation rate of waves. The results of FE-simulations can then be compared with the preliminarily computed characteristics of the biosensor. If a characteristic of the biosensor can be well computed both with the harmonic and finite element methods, the harmonic method is preferable because of its computational efficiency.

2 Statement of the basic model

We consider linear material laws for solids (see [6]) and neglect nonlinear terms in the description of the fluid. This is reasonable because displacements and velocities are very small for the structure under consideration.

2.1 Basic equations for the layers

Let u_1 , u_2 , and u_3 be the displacements in x_1 , x_2 , and x_3 directions, respectively; v_1 , v_2 , and v_3 the velocity components; p the pressure; ρ the density. Open regions occupied by the fluid, the aptamer-fluid layer, the gold layer, the guiding layer, and the substrate are denoted by Ω with the subscripts f , a , $gold$, $guid$, and s , respectively.

The constitutive relations for the piezoelectric substrate in the case of small deformations are of the form:

$$\sigma_{ij} = C_{ijkl}\varepsilon_{kl} - e_{kij}E_k, \quad (1)$$

$$D_i = \epsilon_{ij}E_j + e_{ikl}\varepsilon_{kl}. \quad (2)$$

Here, σ_{ij} and ε_{kl} are the stress and the strain tensors, D_i and E_i denote the electric displacement and the electric field; ϵ_{kl} , e_{kij} , and C_{ijkl} denote the material dielectric tensor, the stress piezoelectric tensor, and the elastic stiffness tensor, respectively. The corresponding governing equations for the displacements and the electric potential read:

$$\rho u_{i\,tt} - C_{ijkl} \frac{\partial^2 u_l}{\partial x_j \partial x_k} + e_{kij} \frac{\partial^2 \varphi}{\partial x_k \partial x_j} = 0 \quad \text{in } \Omega_s, \quad (3)$$

$$\epsilon_{ij} \frac{\partial^2 \varphi}{\partial x_i \partial x_j} + e_{ikl} \frac{\partial^2 u_l}{\partial x_i \partial x_k} = 0 \quad \text{in } \Omega_s, \quad (4)$$

where φ is the electric potential such that $E_i = \partial\varphi/\partial x_i$.

The gold layer is conductor so that there is no electric field inside it. The electric field inside the guiding layer is also neglected because of its low electric permeability coefficient. Therefore, the equation (4) for the electric potential disappears and these two media are described by the equation of the form:

$$\rho u_{i\,tt} - C_{ijkl} \frac{\partial^2 u_l}{\partial x_j \partial x_k} = 0 \quad \text{in } \Omega_{guid} \text{ and } \Omega_{gold}. \quad (5)$$

In the fluid layer, the Stokes and mass conservation equations hold:

$$\varrho v_{it} - \nu \Delta v_i - \left(\zeta + \frac{\nu}{3}\right) \frac{\partial}{\partial x_i} \operatorname{div} \vec{v} + \frac{\partial}{\partial x_i} p = 0, \quad (6)$$

$$\varrho_t + \frac{\partial}{\partial x_i} (\varrho v_i) = 0, \quad (7)$$

where ν and ζ are the dynamic and volume viscosities of the fluid, respectively. For weakly compressible fluids the following substitutive equation holds (see [7]):

$$\varrho(p) \approx \varrho_0 + \left. \frac{\partial \varrho}{\partial p} \right|_\varepsilon (p - p_0). \quad (8)$$

Here $\left. \frac{\partial \varrho}{\partial p} \right|_\varepsilon$ means the density change under a constant entropy, ϱ_0 denotes $\varrho(p_0)$. Substituting (8) into (6) and (7) and neglecting the second order terms, we obtain the following governing equations for the fluid:

$$\varrho_0 v_{it} - \nu \Delta v_i - \left(\zeta + \frac{\nu}{3}\right) \frac{\partial}{\partial x_i} \operatorname{div} \vec{v} + \frac{\partial}{\partial x_i} p = 0 \quad \text{in } \Omega_f, \quad (9)$$

$$\gamma p_t + \frac{\partial}{\partial x_i} v_i = 0 \quad \text{in } \Omega_f, \quad (10)$$

where $\gamma = \frac{1}{\varrho_0} \left. \frac{\partial \varrho}{\partial p} \right|_\varepsilon$ is the compressibility of the fluid.

A special homogenization technique developed in [2] is used to treat the aptamer-fluid structure. The initial bristle-like structure surrounded by the fluid is replaced by an averaged material whose properties are derived as the number of bristles goes to infinity whereas their thickness goes to zero but the height remains constant. Thus, we end up with a new layer whose thickness is equal to the height of the aptamer. The governing equation for this layer reads (see [2] and [5]):

$$\varrho u_{itt} - \hat{C}_{ijkl} \frac{\partial^2 u_l}{\partial x_j \partial x_k} - \hat{P}_{ijkl} \frac{\partial^2 u_{tl}}{\partial x_j \partial x_k} = 0 \quad \text{in } \Omega_a, \quad (11)$$

Here, the term containing the tensor \hat{P} describes the viscous damping that originates from the fluid part of the bristle structure. The term containing \hat{C} represents elastic stresses. The density ϱ is a weighted combination of the density of the fluid and the density of the aptamer. The tensors \hat{P} and \hat{C} are computed with FE-method using an analytical representation of solutions of the so-called cell equation which arises in homogenization theory.

2.2 Interface conditions

Figure 2 represents a cross section of the biosensor by the plane $x_2 = \text{const}$. The interfaces between the layers are denoted by Γ_1 , Γ_2 , Γ_3 , and Γ_4 . Here and below, the superscripts *s*, *guid*, *gold*, *a*, and *f* indicate the relation to the substrate, guiding layer, gold layer, aptamer layer, and fluid, respectively.

The continuity of the displacements and the equilibrium of the normal pressures must hold on the interface between every two neighboring solid layers (the averaged aptamer-fluid layer is considered as a solid one). Moreover, the electric displacement and the tangent component of the electric field in the substrate must be zero on Γ_1 because the electric permeability of the guiding layer is small. Therefore, the following conditions hold on the interfaces: i) on Γ_1 :

$$u_i^s = u_i^{\text{guid}}, \quad (12)$$

$$C_{i3kl}^s \frac{\partial u_l^s}{\partial x_k} - e_{ki3}^s \frac{\partial \varphi^s}{\partial x_k} = C_{i3kl}^{\text{guid}} \frac{\partial u_l^{\text{guid}}}{\partial x_k}, \quad (13)$$

$$\epsilon_{3j}^s \frac{\partial \varphi^s}{\partial x_j} + e_{3kl}^s \frac{\partial u_l^s}{\partial x_k} = 0, \quad (14)$$

$$\frac{\partial \varphi^s}{\partial x_1} = 0. \quad (15)$$

ii) on Γ_2 :

$$u_i^{\text{guid}} = u_i^{\text{gold}}, \quad (16)$$

$$C_{i3kl}^{\text{guid}} \frac{\partial u_l^{\text{guid}}}{\partial x_k} = C_{i3kl}^{\text{gold}} \frac{\partial u_l^{\text{gold}}}{\partial x_k}. \quad (17)$$

iii) on Γ_3 (see [5] for the expression of the pressure in the homogenized layer):

$$u_i^{\text{gold}} = u_i^a, \quad (18)$$

$$C_{i3kl}^{\text{guid}} \frac{\partial u_l^{\text{guid}}}{\partial x_k} = \hat{C}_{i3kl}^a \frac{\partial u_l^a}{\partial x_k} + \hat{P}_{i3kl}^a \frac{\partial u_{tl}^a}{\partial x_k}. \quad (19)$$

The conditions on the interface between the aptamer layer and the fluid include the no-slip assumption and the equilibrium of the pressures. Thus, we have on Γ_4 :

$$\frac{\partial u_i^a}{\partial t} = v_i^f, \quad (20)$$

$$\hat{C}_{i3kl}^a \frac{\partial u_l^a}{\partial x_k} + \hat{P}_{i3kl}^a \frac{\partial u_{tl}^a}{\partial x_k} = \quad (21)$$

$$- p^f \delta_{i3} + \nu \left(\frac{\partial v_i^f}{\partial x_3} + \frac{\partial v_3^f}{\partial x_i} \right) + \left(\zeta - \frac{2}{3} \nu \right) \delta_{i3} \operatorname{div} \vec{v}^f.$$

3 Finite element model

3.1 Adjustment of the basic model

The FE-model extends the basic model described above, by taking into account additionally two alternated groups of the electrodes and a damping area (see Figure 2) which surrounds the biosensor and serves for suppressing wave reflections on the side and bottom faces.

The electrodes are typically made of gold. Therefore, they can be accounted for by the linear elasticity equation (5) considered in Ω_e , where Ω_e is the region occupied by the input and output electrodes.

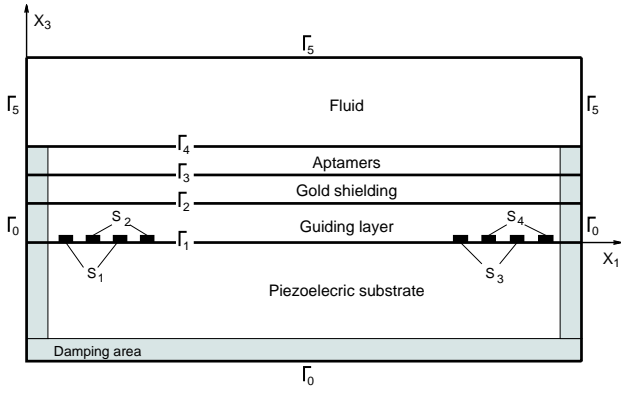


Figure 2. Cross section of the biosensor.

The damping region includes a bottom strip and four side strips. In practice, some adhesive material like silicon caoutchouc is stuck to the side and bottom faces of the device. Accounting for the damping is done by adding the term $-\text{div}(\beta(x)\nabla u_{i,t})$ to equations (3), (5), and (11), where $\beta(x)$ is a piecewise-linear function which is equal to zero outside of the damping region and grows up to some $\beta_0 > 0$ towards the side and bottom boundaries of the sensor.

3.2 Boundary conditions

Since the FE-model is spatially bounded and the electrodes are taken into account, conditions on the external boundaries Γ_0 and Γ_5 as well as conditions on the electrodes S_1 , S_2 , S_3 , and S_4 (see Figure 2) should be specified in addition to the interface conditions (12)–(21).

The following boundary conditions are posed:

- Absence of forces on Γ_0 .
- Continuity of the displacements on the boundaries of the input and output electrodes.
- Equilibrium of the pressures on the boundaries of the input and output electrodes.
- Dirichlet conditions for the electric potential: $\varphi|_{S_1} = 0$, $\varphi|_{S_2} = V(t)$, $\varphi|_{S_4} = 0$, and a conductivity condition for the output electrodes: $\varphi|_{S_3} = C(t)$. Here, $V(t)$ is a prescribed exciting voltage, whereas $C(t)$ is the output voltage to be determined from the equations.
- No-slip condition on Γ_5 : $\vec{v} = 0$.

Note that the condition (20) is the most difficult to fulfill because it is not embedded into the weak formulation of the model equations. The following method from [8] is used to treat the problem. A new variable w is introduced and the variable transformation

$$\vec{u} = \vec{u}_0 + \int_0^t \vec{w} d\tau \quad (22)$$

in all the equations and the boundary conditions is performed. The condition (20) converts into the natural condition $w_i^a = v_i^f$ on Γ_4 .

3.3 Implementation features

The gold and aptamer layers are very thin comparing with the thickness of other layers and the horizontal dimensions of the biosensor. The thickness of the gold layer is about 40 nm, the thickness of the aptamer layer lies in the range of several nanometers. Thus, the displacements in these layers are assumed to be constant in x_3 . This allows us to simplify the volume integrals describing the gold and aptamer layers in the weak formulation of the problem: the volume integrals degenerate to the plane integrals multiplied by the layer thickness. Numerically, this means that planar finite elements can be used for these layers.

4 Harmonic analysis (dispersion relations)

4.1 Description of the algorithm

The algorithm is described here quite briefly (see [4] and [5] for more details). It is assumed that all the layers are infinite in x_1 and x_2 directions, the top fluid layer and the bottom substrate layer are semi-infinite in x_3 direction. The electrodes are not taken into account.

We are looking for solutions describing plain waves propagating in x_1 direction, which means that the displacements in the solid layers, the velocities in the fluid, and the electric potential in the substrate are of the form:

$$u_i(x_1, x_3) = a_i(x_3) \cos(\kappa x_1 - \omega t) + b_i(x_3) \sin(\kappa x_1 - \omega t), \quad (23)$$

$$v_i(x_1, x_3) = c_i(x_3) \cos(\kappa x_1 - \omega t) + d_i(x_3) \sin(\kappa x_1 - \omega t), \quad (24)$$

$$\varphi(x_1, x_3) = f(x_3) \cos(\kappa x_1 - \omega t) + g(x_3) \sin(\kappa x_1 - \omega t), \quad (25)$$

where κ is the wave number and ω is the circular frequency which is equal to the frequency of the voltage applied to the input electrodes in our case. Substitute (23) and (25) into (3) and (4) for the substrate; (23) into (5) and (11) for non-piezoelectric layers and for the aptamer layer; and (24) into (9) for the fluid layer. Equating the coefficients on \cos and \sin , we obtain a system of ordinary linear differential equations for the coefficients a_i , b_i , c_i , d_i , f , g in each layer. Solving these systems for every layer, we obtain the representation of the functions a_i , b_i , c_i , d_i , f , g in the following form (only the expression for the function $\vec{a} = (a_1, a_2, a_3)$ is given here because the form of the other functions is similar):

$$\vec{a}(x_3) = \sum_j D^j \vec{h}^j e^{\lambda^j \kappa x_3}, \quad (26)$$

where D^j are arbitrary coefficients, λ^j and \vec{h}^j are eigenvalues and eigenvectors of the matrix of the corresponding

system of differential equations. For the semi-infinite fluid and substrate layers, only terms decreasing towards x_3 for the fluid and towards $-x_3$ for the substrate, i.e. terms with negative $Re\lambda^j$ for the fluid and positive $Re\lambda^j$ for the substrate, are kept.

Every layer has its own set of coefficients D^j , eigenvalues λ^j , and eigenvectors \vec{h}^j . To find any particular travelling wave solution in the whole structure we need to determine the coefficients D^j for each layer, which is being done by substituting the expressions of the form (26) for the functions a_i, b_i, c_i, d_i, f, g into (23)–(25) and then the resulting functions u_i, v_i, φ into the interface conditions (12)–(21). Since all the expressions (12)–(21) are linear, this yields a homogeneous system of linear equations for unknown coefficients D^j . Denote by $G(\omega, \kappa)$ the matrix of this system. Fixing the circular frequency ω and denoting the unknown wave velocity by $V = \omega/\kappa$, we can consider G as a function of V . The wave velocity is feasible if and only if the system has a nontrivial solution, which is equivalent to the condition: $\det \left[\overline{G}^T(V)G(V) \right] = 0$. The last equation can be easily solved because the computation of the left-hand-side runs very quickly even on an ordinary computer. Usually, several roots are being found, which corresponds to different types of waves propagating with different velocities. When this method is applied to the modelling of the biosensor, the root corresponding to the shear wave (that is only $u_2 \neq 0$) is to be chosen.

5 Simulation results

Both methods are used complementary for the simulation of the biosensor.

First, the harmonic approach was applied to characterize shear waves feasible for the biosensor. The wavelength obtained at this stage was then used to choose the number of x_1 -subdivisions in the FE-model: there should be at least five subdivisions per wavelength. Besides, the width of the electrode plus the distance between the neighboring electrodes should be equal to the wavelength. Moreover, the harmonic approach was used to identify the degree of decay of waves in the substrate and fluid layers. This information was used to introduce semi-infinite finite elements whose shape functions decay exponentially according to the attenuation of waves in the substrate and fluid.

At the next stage, the FE-model was used to account for fine details of the biosensor. Figure 3 shows the second component of the velocity in the cutting plane passing through the top face of the substrate. Figure 4 shows a vertical cross-section of the graph from Figure 3 by the plane $x_2 = l/2$, where l is the x_2 -size of the biosensor.

A number of simulation varying the frequency from 60 till 120 MHz were done. Figure 5 presents the dependence of the wavelength on the excitation frequency (dispersion relation). The results obtained both with the harmonic approach and through the FE-simulations are compared. A very good agreement is observed.

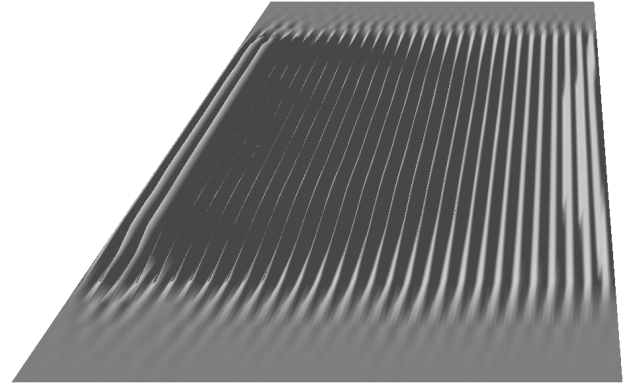


Figure 3. Shear wave profile in the cutting plane passing through the top face of the substrate.

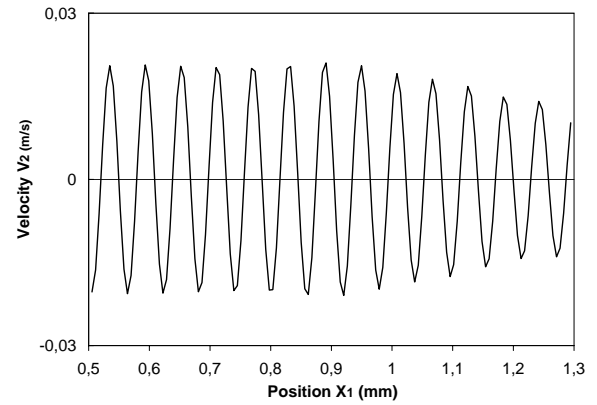


Figure 4. Shear wave profile along the line $x_2 = l/2$, $x_3 = 0$, where l is the x_2 -size of the biosensor.

Figure 6 shows an important characteristic of the biosensor: the efficiency of wave excitation against the number of the electrode pairs. Note that there exists an optimal value which is specific for other constructive and operating parameters of the biosensor.

6 Conclusion

A three-dimensional model of the biosensor is developed. Two approaches to the treatment of the model are outlined. The methods are considered as complementary tools that should be applied together. The method based on the construction of travelling waves in multi-layered structures allows us to find many basic parameters of the biosensor very promptly, i.e. without involving long computations. Thus, the wave length and the velocity profile can be found at this stage. These preliminary values can then be used to adjust the FE-model, to estimate the number of necessary elements, which enables to simulate the biosensor more accurately. On the other hand, the dispersion relations can be used for fast verification of results of FE-simulations.

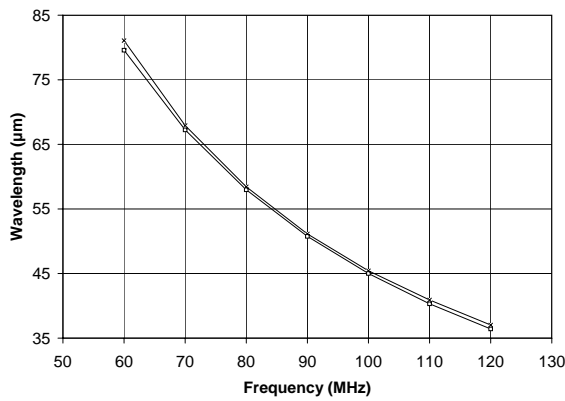


Figure 5. The wavelength depending on the excitation frequency. The lower curve is computed with the harmonic approach, the upper curve is obtained by means of FE-simulations.

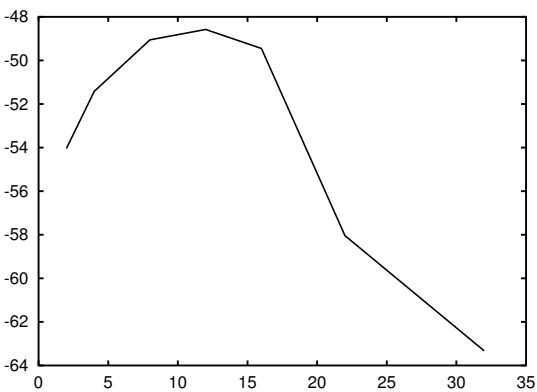


Figure 6. Efficiency of wave excitation (the insertion loss) against the number of the electrode pairs. The insertion loss is defined as $20 \lg(\text{output voltage} / \text{input voltage})$.

The presented methods have been successfully applied to the development of the biosensor at the research center *caesar* at the design stage. The computational results show a good agreement with physical experiments.

References

[1] N. Botkin and V. Turova, Mathematical models of a biosensor. *Applied Mathematical Modelling*, 28, 2004, 573-589.

[2] K.-H. Hoffmann, N. D. Botkin, and V. N. Starovoirov. Homogenization of interfaces between rapidly oscillating fine elastic structures and fluids. *SIAM J. Appl. Math.*, 65(3), 2005, 983-1005.

[3] C. Ashcraft and R. Grimes, SPOOLES: an object-oriented sparse matrix library, *Proc. 9th SIAM Conference on Parallel Processing for Scientific Computing*, San Antonio, USA, 1999.

[4] N.D. Botkin, K.-H. Hoffmann, O. A. Pykhteev, and V.L. Turova, Numerical computation of dispersion relations for multi-layered anisotropic structures, *Proc. Nanotechnology Conference and Trade Show*, Boston, USA, 2004, Vol. 2, 411-414.

[5] N.D. Botkin, K.-H. Hoffmann, O.A. Pykhteev, and V.L. Turova, Dispersion relations for acoustic waves in heterogeneous multi-layered structures contacting with fluids, to appear in *Journal of the Franklin Institute*.

[6] J. Zelenka, *Piezoelectric Resonators and their Applications. Studies in Electrical and Electronic Engineering*, 24, (Amsterdam, Elsevier, 1986).

[7] L. D. Landau and E. M. Lifshitz, *Course of theoretical physics. Vol.6. Fluid mechanics*, (Oxford, Pergamon Press, 1982).

[8] J.L. Lions, *Quelques Methodes de Resolution des Problemes aux Limites non Lineaires*, (Paris, Dunod Gauthier-Villars, 1969).